11. Platinum bipolar stimulating electrodes were lowered 7 mm below the cortical surface 3.3 mm lateral and 2.3 mm posterior to the bregma in barbiturate-anesthetized rats weighing ~300 g and were cemented into place with the use of sterile techniques approved under animal care protocol of the University of California, San Francisco. After 2 weeks of recovery, 250-ms (or a 15-Hz train of six 25-ms) 50-dB sound pressure level tones were paired with 200 ms of NB electrical stimulation in a sound-shielded, calibrated test chamber (5 days per week). Electrical stimulation began either 50 ms after tone onset ($n = 15$) or 200 ms before ($n = 6$). The two timings did not appear to affect plasticity, and data from both groups were pooled. The current level (70 to 150 μA) was chosen to be the minimum necessary to desynchronize the EEG during slow-wave sleep for 1 to 2 s. Stimulation consisted of 100-Hz capacitatively coupled biphasic pulses of 0.1 ms duration. Tonal and electrical stimuli did not evoke any observable behavioral responses (that is, did not cause rats to stop grooming or if sleeping, awaken).
12. Twenty-four hours after the last pairing, animals were anesthetized with pentobarbital and the right auditory cortex was surgically exposed. Parylene-coated tungsten microelectrodes (2 megohms) were lowered 550 μm below the pial surface (layer 4/5), and complete tuning curves were generated with 50-ms pure tones (with 3-ms ramps) presented at 2 Hz to the contralateral ear. The evoked spikes of a small cluster of neurons were collected at each site. To determine the effects of conditioning on the bandwidth of individual neurons, spike waveforms were collected during eight experiments and were sorted offline with software from Brainwave Technologies. Penetration locations were referenced using the cortical vasculature as landmarks. The primary auditory cortex was defined on the basis of its short latency (8- to 20-ms) responses and continuous tonotopy (BF increases from posterior to anterior). Responsive sites that exhibited clearly discontinuous BFs and either long latency responses, an unusually high threshold, or very broad tuning were considered to be non-A1 sites. Penetration sites were chosen to avoid blood vessels while generating a detailed and evenly spaced map. The edges of the map were estimated with the use of a line connecting the nonresponsive and non-A1 sites. Map reorganizations resulted in significant effects on the outline of A1, although no particular pattern was observed. The effect of conditioning on mean bandwidths across all conditions was determined with analysis of variance; pairwise comparisons were analyzed by Bonferroni post-hoc tests.
13. The set of tone frequencies presented at each site was approximately centered on the BF of each site. Thus, during analysis each tuning curve was approximately centered in the stimulus space, and simply blanking the axes and analyzing the sites in random order allowed for tuning curve characterization to be completely blind. With the use of custom analysis software, the tuning curve edges for each site were defined by hand and recorded without the possibility of experimenter bias.
14. S. L. Sally and J. B. Kelly, *J. Neurophysiol.* **59**, 1627 (1988).
15. G. H. Recanzone, C. E. Schreiner, M. M. Merzenich, *J. Neurosci.* **13**, 87 (1993).
16. W. M. Jenkins, M. M. Merzenich, M. T. Ochs, T. Allard, E. Guic-Robles, *J. Neurophysiol.* **63**, 82 (1990).
17. G. H. Recanzone, M. M. Merzenich, W. M. Jenkins, K. A. Grajski, H. R. Dinse, *ibid.* **67**, 1031 (1992).
18. M. P. Kilgard and M. M. Merzenich, unpublished observation.
19. In contrast to the large changes induced by pairing tones with NB stimulation, no significant cortical map reorganizations were observed in previous experiments after tens of thousands of behaviorally irrelevant stimuli were presented over 3 to 5 months (*14, 16*). Additionally, short-term repetition of one frequency without behavioral relevance (habituation) results in a dramatic decrease in A1 responses to that frequency [C. D. Condon and N. M. Weinberger, *Behav. Neurosci.* **105**, 416 (1991)]. These studies suggest that stimulus presentation without behavioral importance does not result in significant map changes. Although it is unlikely to be a contributing factor, we acknowledge that we did not record from animals that experienced extensive stimulus presentation without any NB stimulation.
20. F. Casamenti, G. Deffenu, A. L. Abbamondi, G. Pepeu, *Brain Res. Bull.* **16**, 689 (1986); D. D. Rasmusson, K. Clow, J. C. Szerb, *Brain Res.* **594**, 150 (1992); M. E. Jimenez-Capdeville, R. W. Dykes, A. A. Myasnikov, *J. Comp. Neurol.* **381**, 53 (1997).
21. B. Hars, C. Maho, J. M. Edeline, E. Hennevin, *Neuroscience* **56**, 61 (1993); J. S. Bakin and N. M. Weinberger, *Proc. Natl. Acad. Sci. U.S.A.* **93**, 11219 (1996).
22. The cholinergic neurons of the NB were selectively destroyed by infusion of 2.5 μg of 192 immunoglobulin G–saporin immunotoxin into the right lateral ventricle before the surgery to implant the stimulating electrode. The toxin, an antibody to the low-affinity nerve growth factor receptor linked to a ribosome-inactivating toxin, has been shown to specifically destroy most of the cholinergic neurons of the basal forebrain projecting to the cortex, while sparing the parvalbumin-containing neurons as well as cholinergic neurons that project from the NB to the amygdala [S. Heckers *et al.*, *J. Neurosci.* **14**, 1271 (1994)]. Electrical stimulation of the NB and tone presentation were identical for lesioned and nonlesioned animals. The percent of the cortex responding to a 19-kHz tone after pairing in lesioned animals was not significantly different from that in naïve controls (two-tailed t test, $n = 2$).
23. I. Gritti, L. Mainville, M. Mancia, B. E. Jones, *J. Comp. Neurol.* **383**, 163 (1997).
24. Complex considerations of the network, cellular, and molecular mechanisms responsible for the plasticity observed in our studies are beyond the scope of this report. See M. E. Hasselmo and J. M. Bower, *Trends Neurosci.* **16**, 218 (1993); M. Sarter and J. P. Bruno, *Brain Res. Rev.* **23**, 28 (1997); R. W. Dykes, *Can. J. Physiol. Pharmacol.* **75**, 535 (1997).
25. Supported by NIH grant NS-10414, Hearing Research Inc., and an NSF predoctoral fellowship. We thank C. Schreiner for technical advice and D. Buonomano, H. Mahncke, D. Blake, C. deCharms, C. Schreiner, and K. Miller for helpful comments on the manuscript.

28 October 1997; accepted 23 January 1998

Activation of the OxyR Transcription Factor by Reversible Disulfide Bond Formation

Ming Zheng, Fredrik Åslund, Gisela Storz*

The OxyR transcription factor is sensitive to oxidation and activates the expression of antioxidant genes in response to hydrogen peroxide in *Escherichia coli*. Genetic and biochemical studies revealed that OxyR is activated through the formation of a disulfide bond and is deactivated by enzymatic reduction with glutaredoxin 1 (Grx1). The gene encoding Grx1 is regulated by OxyR, thus providing a mechanism for autoregulation. The redox potential of OxyR was determined to be –185 millivolts, ensuring that OxyR is reduced in the absence of stress. These results represent an example of redox signaling through disulfide bond formation and reduction.

Reactive oxygen species can damage DNA, lipid membranes, and proteins and have been implicated in numerous degenerative diseases (*1*). As a defense, prokaryotic and eukaryotic cells have inducible responses that protect against oxidative damage (*2*). These antioxidant defense systems have been best characterized in *Escherichia coli*, in which the OxyR and SoxR transcription factors activate antioxidant genes in response to H_2O_2 and to superoxide-generating compounds, respectively.

The mechanisms of redox-sensing and the systems that control the redox status of the cell are likely to be coupled. Studies of the thiol-disulfide equilibrium of the cytosol of both prokaryotic and eukaryotic cells indicate that the intracellular environment is reducing, such that protein disulfide bonds rarely occur (*3–5*). The redox potential of the *E. coli* cytosol has been estimated to be approximately –0.26 to –0.28 V (*4, 5*). This reducing environment is maintained by the thioredoxin and the glutaredoxin systems (*6, 7*).

In response to elevated H_2O_2 concentrations, the OxyR transcription factor rapidly induces the expression of *oxyS* (a small, nontranslated regulatory RNA), *katG* (hydrogen peroxidase I), *gorA* (glutathione reductase), and other activities likely to protect the cell against oxidative stress (*2, 8*). Purified OxyR is directly sensitive to oxidation. Only the oxidized form of OxyR can activate transcription in vitro, and footprinting experiments indicate that oxidized and reduced OxyR have different conformations (*9, 10*). Thus, we examined the chemistry of OxyR oxidation and reduction.

No transition metals were detected by inductively-coupled plasma metal ion analysis of two preparations of OxyR (*11*). We also did not observe any change in OxyR activity after denaturation and renaturation in the presence of the metal chelator des-

M. Zheng and G. Storz, Cell Biology and Metabolism Branch, National Institute of Child Health and Human Development, National Institutes of Health, Bethesda, MD 20892, USA.
F. Åslund, Department of Microbiology and Molecular Genetics, Harvard Medical School, Boston, MA 02115, USA.

*To whom correspondence should be addressed. E-mail: storz@helix.nih.gov

ferrioxamine (Fig. 1A), indicating that metal ions and other prosthetic groups are unlikely to be the redox-active center of OxyR. Previous mutational studies suggested that at least one and possibly two of the six cysteine residues in OxyR are critical for activity (*12*). We found that the $Cys^{199} \rightarrow Ser^{199}$ (C199S) mutant strain showed no expression of the OxyR-regulated *oxyS* gene, and the $Cys^{208} \rightarrow Ser^{208}$ (C208S) mutant strain only showed slight expression (Fig. 1B). Thus, both Cys^{199} and Cys^{208} are critical to the activation of OxyR. In addition, an alignment of OxyR homologs shows that only two cysteine residues, corresponding to Cys^{199} and Cys^{208} of *E. coli* OxyR, are conserved (*13*).

To examine the oxidation state of the Cys^{199} and Cys^{208} residues in vitro, we generated an OxyR derivative (OxyR4C → A) carrying Ala substitutions of the other four cysteines. This derivative showed activity identical to the wild-type protein in vivo (Fig. 1B) and in vitro (*14*). We examined the OxyR4C → A protein by matrix-assisted laser desorption/ionization–time-of-flight (MALDI-TOF) mass spectrometry (Fig. 1C). For the reduced protein, two peaks corresponded to fragments containing alkylated Cys^{199} and Cys^{208}. These two peaks completely disappeared for the oxidized protein. Instead, a new peak that corresponded to the sum of the Cys^{199}- and Cys^{208}-containing peptide fragments joined by a disulfide bond, was detected. Quantitative thiol-disulfide titrations also indicated that oxidized OxyR contains one disulfide bond (*15*). We conclude that formation of an intramolecular (*16*) disulfide bond between residues Cys^{199} and Cys^{208} leads to the conformational change that activates the OxyR transcription factor.

Although both Cys^{199} and Cys^{208} were important to OxyR activation, the increased sensitivity of the C199S mutant over the C208S mutant suggested that these two residues are not equivalent. Because the formation of disulfide bonds upon H_2O_2 oxidation has been reported to proceed through the initial oxidation of one Cys through a sulfenic acid intermediate (–SOH) (*17, 18*), we propose that the oxidation of Cys^{199} to –SOH is the first step in OxyR activation (*19*).

OxyR activation by H_2O_2 is a transient phenomenon. In a wild-type background, the amounts of *oxyS* reach a maximum ~10 min after H_2O_2 treatment and then decrease to near basal levels within 60 min after the treatment (Fig. 2A). The amounts of the OxyR protein do not change after the H_2O_2 treatment (*9*), suggesting that oxidized OxyR is deactivated by reduction of the Cys^{199}-Cys^{208} disulfide bond. We generated a set of isogenic strains defective in *gorA* (glutathione reductase), *grxA* (Grx1), *gshA* (glutathione synthetase), *trxB* (thioredoxin reductase), and *trxA* (thioredoxin)—the components of the two main disulfide reduction systems in the cell. We then examined the activity of OxyR. Compared to the wild-type strain, *oxyS* RNA levels were elevated 30 min after H_2O_2 treatment in the *gorA*$^-$, and particularly the *grxA*$^-$ and *gshA*$^-$ mutants. By contrast, the *trxA*$^-$ mutant showed a profile identical to the wild-type strain (*14*), and the *trxB*$^-$ mutant exhibited a more rapid decrease in *oxyS* expression, possibly because of increased Grx1 levels in this strain. Because Grx1 is known to catalyze protein disulfide bond reduction by reduced glutathione (GSH), Grx1 may catalyze OxyR deactivation at the expense of GSH. To test this hypothesis, we incubated oxidized OxyR with purified GSH and Grx1. OxyR activity was completely eliminated within 30 min (Fig. 2B, lane 4). OxyR deactivated in this manner could readily be reactivated by H_2O_2 upon removal of GSH (lane 5). These genetic and biochemical results indicate that OxyR is deactivated through enzymatic disulfide bond reduction by Grx1.

OxyR was initially identified as a sensor for H_2O_2 levels. However, the OxyR-regulated *katG* gene has also been reported to be induced by diamide and *S*-nitrosothiols (*20*). To test the OxyR sensing specificity, we treated cells with H_2O_2, diamide, *S*-nitroso-

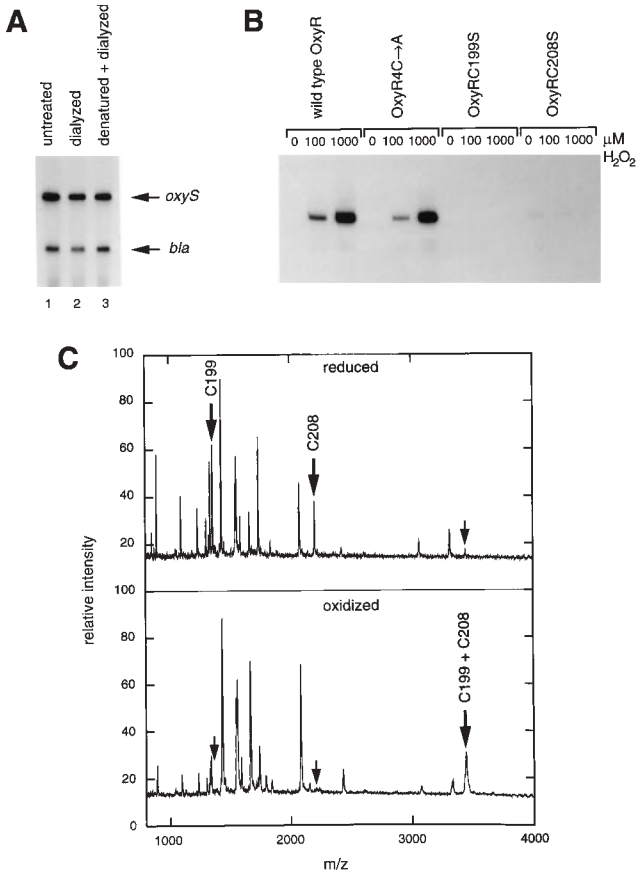

Fig. 1. Direct activation of OxyR. (**A**) The buffer in a sample of OxyR (1 ml of ~0.5 mg/ml) was exchanged by three additions (1 ml) of 6 M guanidine hydrochloride in 0.1 M potassium phosphate (pH 7.0) and concentrated to 50 μl in a Centricon unit (10 kD cutoff, Amicon). Circular dichroism measurements confirmed that the OxyR protein was denatured by the guanidine hydrochloride. An aliquot of denatured OxyR was then renatured by a 6-hour dialysis against three 100-ml volumes of protein purification buffer containing the metal chelator desferrioxamine (0.1 mM, Sigma). Subsequently, equal amounts of an untreated sample (lane 1), a sample dialyzed against 0.1 M potassium phosphate, pH 7.0 (lane 2), and the denatured and dialyzed sample (lane 3) were analyzed by in vitro transcription assays using purified RNA polymerase (U.S. Biochemical) and pAQ17 as a template. OxyR was purified as described (*12*), with the exception that dithiothreitol (DTT) was eliminated from the purification buffer. All transcription reactions (*12*) were carried out with ≤1 μM OxyR to ensure a linear response. (**B**) Strains expressing wild-type OxyR, OxyR4C→A, OxyRC199S, and OxyRC208S (on pUC plasmids) were grown to an optical density at 600 nm (OD_{600}) = 0.2 in LB medium and then treated with 0, 100, or 1000 μM H_2O_2. Total RNA was isolated from samples taken at 10 min, and the amounts of *oxyS* RNA were analyzed by primer extension (5′-CGTTTTCAAGGCCC) (*8*). (**C**) MALDI-TOF spectra for reduced (top) and oxidized (bottom) OxyR4C→A after alkylation and trypsin digestion were taken with a LaserTec Bench-Top (VESTEC) mass spectrometer. All the predicted tryptic fragments could be identified in the 800- to 4000-dalton region, and the mass of each observed fragment differed from its theoretical value by <1 dalton. To prepare the samples, we first alkylated reduced and oxidized OxyR4C→A [100 μl of 0.5 mg/ml, purified as in (A) after extraction from inclusion bodies] by a 10-min incubation with iodoacetamide (1 μl of 1 M in H_2O, Sigma). Trypsin (1 μl of 1 mg/ml, Promega) was added to the alkylated protein (25 μl of ~0.5 mg/ml), and the mixture was incubated overnight at 37°C. Subsequently, 1 μl of the digestion product was added to 3 μl of saturated 2,5-dihydroxybenzoic acid (Aldrich) in a 2:1 0.1% trifluoroacetic acid/acetonitrile solvent mixture, and 1 μl of this mixture was loaded onto the sample pin of the spectrometer. The generation of reduced OxyR4C→A protein and all subsequent manipulations were carried out in an anaerobic chamber (Coy Laboratory) filled with 5% H_2 and 95% N_2.

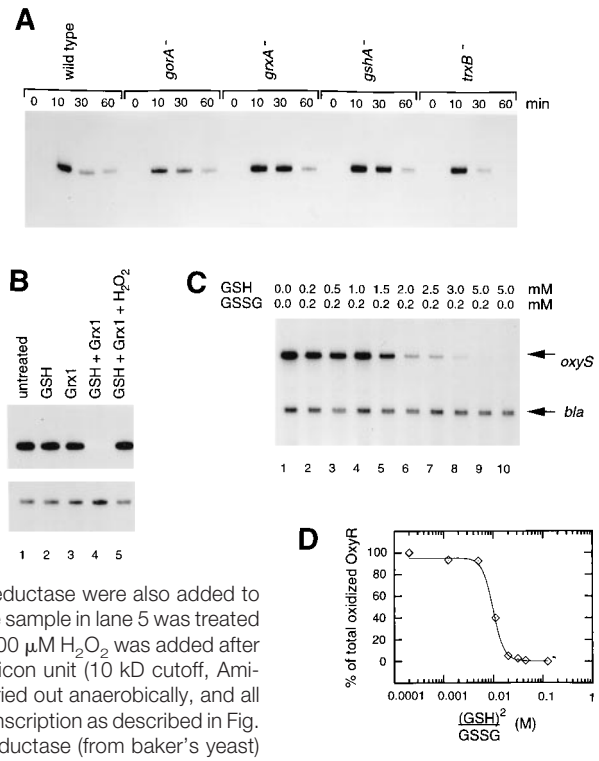

Fig. 2. OxyR deactivation by Grx1. (**A**) The *gorA*$^-$, *grxA*$^-$, *gshA*$^-$, *trxB*$^-$, and *trxA*$^-$ mutant alleles (*27*) were moved into MC4100 by P1 transduction (generating GSO48-GSO52). The strains were grown to OD_{600} = 0.2 in minimum M63 medium supplemented with 0.2% glucose and 0.002% vitamin B1 and then treated with 200 μM H_2O_2. Total RNA isolated from samples taken at 0, 10, 30, and 60 min was analyzed by primer extension as in Fig. 1. The data shown is representative of the average (2.3, 1.8, 0.5, 0.5, 2.4, and 2.0% decay/min for wild type, *gorA*$^-$, *grxA*$^-$, *gshA*$^-$, *trxB*$^-$, and *trxA*$^-$, respectively) of 10 experiments. (**B**) Samples of purified OxyR (0.8 μM) were incubated with 5 mM GSH (lane 2), 10 μM Grx1 (lane 3), 5 mM GSH and 10 μM Grx1 (lane 4) for 30 min. NADPH (0.5 mM) and 10 μg/ml glutathione reductase were also added to the samples in lanes 2 through 5. The sample in lane 5 was treated as described for lane 4 except that 200 μM H_2O_2 was added after the GSH was removed with a Centricon unit (10 kD cutoff, Amicon). The entire experiment was carried out anaerobically, and all samples were analyzed by in vitro transcription as described in Fig. 1. NADPH, GSH, and glutathione reductase (from baker's yeast) were purchased from Sigma, and Grx1 was kindly provided by J. Bushweller and A. Holmgren. The results shown are representative of four independent experiments. (**C**) The indicated amounts of GSH and GSSG were incubated with 0.8 μM OxyR and 10 μM Grx1 at pH 7 and 27°C for at least 72 hours. The samples were then added to RNA polymerase and assayed by in vitro transcription. All steps were carried out anaerobically. (**D**) The intensities of the *oxyS* and *bla* bands in (C) were measured by a PhosporImager (Molecular Dynamics) and then converted to OxyR (oxidized) concentration, using a calibration curve obtained from a control experiment in which a total of 0.8 μM OxyR composed of defined amounts of oxidized and reduced OxyR was assayed by in vitro transcription under the same conditions used for the titration. The diamonds correspond to experimental data, and the solid line is the theoretical fit {% oxidized OxyR = $K_{eq}/(K_{eq} + [GSH]^8/[GSSG]^4)$} based on Eq. 1. The redox potential of –185 ± 5 mV is derived from three independent experiments.

cysteine (SNO-Cys), nitrite, hydrazine and its derivatives, hypochlorous acid, and oxidized lipoic acid (*14*). Only H_2O_2 and diamide activated OxyR in the wild-type strain, and diamide activation was only observed at concentrations greater than 100 μM (Fig. 3A). SNO-Cys did activate OxyR in a *gshA*$^-$ strain, but activation by SNO-Cys was always lower than the activation by H_2O_2 (Fig. 3A). In vitro, diamide, SNO-Cys, and oxidized glutathione (GSSG) all partially activated OxyR but to significantly lower amounts than did H_2O_2 (Fig. 3B). Thus, although diamide and SNO-Cys might react with the two critical cysteines in OxyR, the transcription factor seems to have evolved to specifically sense peroxides.

The reversible reaction between OxyR and GSH/GSSG (Fig. 3B) allowed us to measure the redox potential of OxyR. We incubated OxyR with defined concentrations of GSH/GSSG and then measured the relative amounts of oxidized (activated) OxyR by in vitro transcription assays (Fig. 2C). When the GSH:GSSG ratio in the buffer exceeded 5:1 (between lanes 4 and 6), there was a sudden and substantial drop in transcription activity. This titration data (Fig. 2D) was best fit by assuming a concerted four-monomer oxidation and reduction (Eq. 1), which is consistent with the observation that OxyR is a tetramer in solution (*21*).

$$\mathrm{OxyR(ox)} + 8\,\mathrm{GSH} \xleftrightarrow{\mathrm{Grx1}} \mathrm{OxyR(red)} + 4\,\mathrm{GSSG} \quad (1)$$

The extracted equilibrium constant for Eq. 1 was used to calculate the redox potential of OxyR (*22*). The derived value of –185 ± 5 mV is about 90 mV higher than the estimated redox potential of the *E. coli* cytosol (–280 mV) (*4*, *5*), providing a ther-

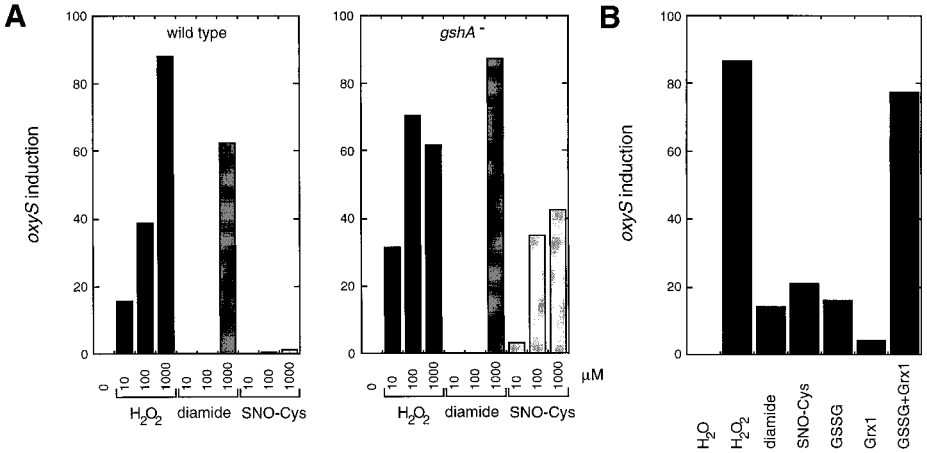

Fig. 3. Specificity of OxyR oxidation. (**A**) The wild-type (MC4100) and *gshA*$^-$ (GSO49) strains were grown in minimal medium as in Fig. 2 and then treated with 10, 100, or 1000 μM H_2O_2, diamide (Sigma), and SNO-Cys [synthesized according to (*28*)]. Total RNA was isolated from cells collected after 10 min, and primer extension assays were carried out as in Fig. 1. The *oxyS* levels were quantified on a PhosphorImager and plotted. (**B**) Purified OxyR was reduced by overnight treatment with 0.1 mM DTT, which was then removed by dialysis (Pierce dialysis cassette). The samples (0.8 μM) were then treated with 200 μM H_2O_2, 200 μM diamide, 200 μM SNO-Cys, 200 μM GSSG (Sigma), 10 μM Grx1, and 200 μM GSSG plus 10 μM Grx1 for 5 min and assayed by in vitro transcription. The entire experiment was carried out anaerobically. The in vivo and in vitro assays were both repeated at least twice; representative experiments are shown.

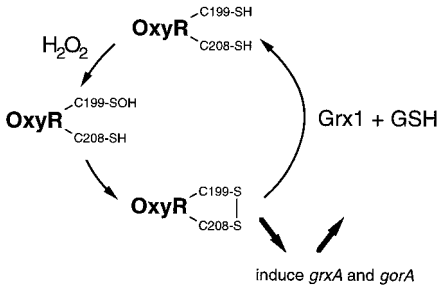

Fig. 4. Model for OxyR activation and deactivation. Upon exposure to H_2O_2, the Cys^{199} residue of OxyR is first oxidized to a sulfenic acid. This reactive intermediate subsequently reacts with Cys^{208} to form a stable disulfide bond locking OxyR in an activated form. Oxidized OxyR is rereduced by disulfide bond reduction by the glutaredoxin system. Because OxyR activates the transcription of *grxA* (Grx1) and *gorA* (glutathione reductase), the entire response is autoregulated.

modynamic basis for the observation that OxyR is predominantly reduced (deactivated) under normal conditions. The redox potential of OxyR is also higher than the potential of all the known disulfide reductases in *E. coli* (*7*). Thus, thioredoxin should also be capable of reducing OxyR, and indeed, we found that the purified enzyme deactivates OxyR in vitro (*23*). Because the OxyR protein is eventually reduced in *gorA*$^-$, *grxA*$^-$, and *gshA*$^-$ mutant strains, it is also likely that the other disulfide bond reduction systems contribute to the deactivation of OxyR in vivo.

Interestingly, an examination of the promoter region of the *grxA* gene revealed a sequence that showed an 85% match to an OxyR DNA-binding consensus sequence (*10*). We examined the levels of the *grxA* message by primer extension and found that, as previously observed for *gorA*, the expression of *grxA* is induced by H_2O_2 in an OxyR-dependent manner (*24*). Deoxyribonuclease I (DNase I) footprinting experiments also showed that the OxyR footprint precisely overlaps the predicted OxyR binding site (*24*). These results indicate that the OxyR response is autoregulated; OxyR activation by H_2O_2 leads to the induction of activities that trigger the OxyR deactivation pathway.

We have provided evidence that the molecular event of redox signaling by OxyR is disulfide bond formation and reduction (Fig. 4). Two features of OxyR are likely to contribute to its sensitivity to H_2O_2. First, the oxidation and reduction of OxyR tetramers appears to be cooperative. Second, we suggest that the Cys^{199} residue is poised to react with H_2O_2. A comparison of OxyR homologs reveals that two basic residues flanking Cys^{199} are absolutely conserved (*13*). These residues could enhance the reactivity of Cys^{199} toward peroxides by stabilizing the thiolate form of this cysteine (Cys^{199}-S$^-$) or by protonating the leaving group (–OH) of H_2O_2, or both.

OxyR induction of Grx1 and glutathione reductase ensures that the transcription factor is only activated for a defined period of time and may also be a mechanism for cells to maintain redox homeostasis. A drop in the GSH:GSSG ratio could lead to OxyR activation resulting in the induction of the enzymes that restore the redox balance. Because GSH:GSSG ratios vary significantly from one intracellular compartment to another in eukaryotic cells, a variety of cellular processes, including signal transduction and transport, may be modulated by reversible disulfide bond formation.

The redox potential of –185 mV determined for OxyR is substantially higher than the redox potential of –285 mV reported for the SoxR transcription factor (*25*). We propose that whereas the activity of OxyR is responsive to the thiol-disulfide redox status of the cell, the activity of SoxR is responsive to reduced and oxidized nicotinamide adenine dinucleotide phosphate (NADPH/NADP$^+$, respectively) levels in the cell. In general, the difference in the redox potential of the two major intracellular redox buffers (GSH/GSSG and NADPH/NADP$^+$) (*4*) should allow for the regulation of proteins with chemically diverse redox centers.

REFERENCES AND NOTES

1. B. Halliwell and J. M. C. Gutteridge, *Free Radicals in Biology and Medicine* (Clarendon Press, Oxford, 1989).
2. D. J. Jamieson and G. Storz, in *Oxidative Stress and the Molecular Biology of Antioxidant Defenses*, J. G. Scandalios, Ed. (Cold Spring Harbor Laboratory Press, Cold Spring Harbor, NY, 1997), pp. 91–115; B. González-Flecha and B. Demple, in *Reactive Oxygen Species in Biological Systems: An Interdisciplinary Approach*, D. L. Gilbert and C. A. Colton, Eds. (Plenum, New York, in press).
3. G. E. Schultz and R. H. Schirmer, *Principles of Protein Structure* (Springer-Verlag, New York, 1979); J. M. Thornton, *J. Mol. Biol.* **151**, 261 (1981); C. Branden and J. Tooze, *Introduction to Protein Structure* (Garland, New York, 1991).
4. H. F. Gilbert, *Adv. Enzymol. Relat. Areas Mol. Biol.* **63**, 69 (1990).
5. C. Hwang, A. J. Sinskey, H. F. Lodish, *Science* **257**, 1496 (1992).
6. A. I. Derman, W. A. Prinz, D. Belin, J. Beckwith, *ibid.* **262**, 1744 (1993); W. A. Prinz, F. Åslund, A. Holmgren, J. Beckwith, *J. Biol. Chem.* **272**, 15661 (1997).
7. F. Åslund, K. D. Berndt, A. Holmgren, *J. Biol. Chem.* **272**, 30780 (1997).
8. S. Altuvia, D. Weinstein-Fischer, A. Zhang, L. Postow, G. Storz, *Cell* **90**, 43 (1997).
9. G. Storz, L. A. Tartaglia, B. N. Ames, *Science* **248**, 189 (1990).
10. M. B. Toledano *et al.*, *Cell* **78**, 897 (1994).
11. Two samples of OxyR (15 μM) were analyzed by the Chemical Analysis Laboratory at the University of Georgia. No transition metals were detected at a sensitivity of ≤5 pM.
12. I. Kullik, M. B. Toledano, L. A. Tartaglia, G. Storz, *J. Bacteriol.* **177**, 1275 (1995).
13. *Escherichia coli* (J04553, residues 191-208), LLMLEDGH**C**LRDQAMGF**C**; *Erwinia carotovora* (U74302), LLMLEDGH**C**LRDQAMGF**C**; *Haemophilus influenzae* (U49355), MLMLDDGH**C**LRNQALDY**C**; *Xanthomonas campestris* (U94336), LLLLEDGH**C**LRDQALDV**C**; *Mycobacterium leprae* (L01095), LLLLDEGH**C**LRDQTLDI**C**; *Acinetobacter calcoaceticus* (X88895), LMLLEEGH**C**LRDHALSA**C** (*26*).
14. M. Zheng, F. Åslund, G. Storz, data not shown.
15. We carried out 5,5′-dithiobis-(2-nitrobenzoic acid) and 2-nitro-5-thiosulfobenzoate titrations under denaturing conditions as described [P. W. Riddles, R. L. Blakeley, B. Zerner, *Anal. Biochem.* **94**, 75 (1979); T. W. Thannhauser, Y. Konishi, H. A. Scheraga, *ibid.* **138**, 181 (1984)]. For reduced OxyR4C→A, 1.8 equivalents of –SH and 0.1 equivalents of S-S were detected, whereas 0.2 equivalents of –SH and 0.9 equivalents of S-S were detected for the oxidized protein.
16. Mass spectrometry (MALDI-TOF) of oxidized, denatured OxyR revealed a major peak at 34.3 ± 0.1 kD and a minor peak at 17.1 ± 0.1 kD, corresponding to the singly- and doubly-charged OxyR monomer (theoretical mass of 34.28 kD), respectively.
17. J. L. Kice, *Adv. Phys. Org. Chem.* **17**, 65 (1980); A. Claiborne, H. Miller, D. Parsonage, R. P. Ross, *FASEB J.* **7**, 1483 (1993).
18. F. A. Davis and R. L. Billmers, *J. Am. Chem. Soc.* **103**, 7016 (1981); H. R. Ellis and L. B. Poole, *Biochemistry* **36**, 13349 (1997).
19. When we examined the trypsin-digested C208S mutant protein by mass spectrometry, we observed a 2614 dalton peak for the oxidized but not for the reduced C208S protein. The mass of this peak corresponds to that of two Cys^{199}-containing fragments linked via a thiosulfinate functional group, which would be formed by a sulfenic acid condensation reaction [2 Cys^{199}-SOH → Cys^{199}-S(O)S-Cys^{199} + H_2O] [(*17*); E. Block and J. O'Connor, *J. Am. Chem. Soc.* **96**, 3929 (1974); F. A. Davis, L. A. Jenkins, R. L. Billmers, *J. Org. Chem.* **51**, 1033 (1986)].
20. C. T. Privalle and I. Fridovich, *J. Biol. Chem.* **265**, 21966 (1990); A. Hausladen, C. T. Privalle, T. Keng, J. DeAngelo, J. S. Stamler, *Cell* **86**, 719 (1996).
21. I. Kullik, J. Stevens, M. B. Toledano, G. Storz, *J. Bacteriol.* **177**, 1285 (1995).
22. The equilibrium constant K_{eq} extracted from the redox titration data shown in Fig. 2C was used to calculate the redox potential of OxyR according to the Nernst equation:

$$E = E^0 + 2.303(RT/nF) \cdot \log K_{eq}$$

where E is the redox potential of OxyR in reference to the normal hydrogen electrode, E^0 is the standard potential of GSH [–240 mV (*7*)], R is the gas constant, T is the temperature, n is the number of electrons transferred (eight electrons in the case of OxyR), and F is the Faraday constant.
23. OxyR reduction by thioredoxin reductase and thioredoxin was carried out essentially the same as the reduction described in Fig. 2B, except that 10 μg/ml *E. coli* thioredoxin reductase (Imco) and 10 μM *E. coli* thioredoxin (Imco) were used in place of glutathione reductase, Grx1, and GSH.
24. The OxyR-regulated transcription start was mapped to an A residue 23 nucleotides upstream of the AUG. The extent of the OxyR DNase I footprint on both strands is underlined, and the matches to the OxyR binding site consensus (*10*) are capitalized on the following sequences. Top strand: 5′- gtgtttaacagt-tATAGcTtttAgCaATtaatgcaAcAGgTtaaAcCTActttc-agcgaa; bottom strand: 3′- cacaaattgtcaaTATC-gAaaaTcGtTAattacgtTgTCcAattTgGATgaaagtcgctt. The same transcription start and OxyR binding site were recently identified [K. Tao, *J. Bacteriol.* **179**, 5967 (1997)].
25. H. Ding, E. Hidalgo, B. Demple, *J. Biol. Chem.* **271**, 33173 (1996); P. Gaudu and B. Weiss, *Proc. Natl. Acad. Sci. U.S.A.* **93**, 10094 (1996); E. Hidalgo, H. Ding, B. Demple, *Cell* **88**, 121 (1997).
26. Single-letter abbreviations for the amino acid residues are as follows: A, Ala; C, Cys; D, Asp; E, Glu; F, Phe; G, Gly; H, His; I, Ile; K, Lys; L, Leu; M, Met; N, Asn; P, Pro; Q, Gln; R, Arg; S, Ser; T, Thr; V, Val; W, Trp; and Y, Tyr.
27. N. K. Davis, S. Greer, M. C. Jones-Mortimer, R. N. Perham, *J. Gen. Microbiol.* **128**, 1631 (1982); J. T. Greenberg and B. Demple, *J. Bacteriol.* **168**, 1026 (1986); M. Russel and A. Holmgren, *Proc. Natl. Acad. Sci. U.S.A.* **85**, 990 (1988); M. Russel and P. Model, in *Thioredoxin and Glutaredoxin Systems: Structure and Function*, A. Holmgren, C. I. Brändén, H. Jörnvall, B.-M. Sjöberg, Eds. (Raven Press, New York, 1986), pp. 331–337.
28. J. S. Stamler and J. Loscalzo, *Anal. Chem.* **64**, 779 (1992).

29. We thank C. Wu and C. Klee for the use of the MALDI mass spectrophotometer and Pharmacia Smart system, C. Vinson for use of the spectropolarimeter, L. Poole and J. Beckwith (grant GM-41883) for experiments conducted by M.Z. and F.A. in their laboratories, and J. Bushweller, B. Demple, A. Eisenstark, A. Holmgren, and M. Russel for *E. coli* strains, plasmids, and purified Grx1. We also appreciate the advice of J. Beckwith, L. Poole, and W. Prinz, and the editorial comments of J. Beckwith, C. Dismukes, R. Klausner, L. Poole, C. Wu, Y.-L. Wu, and M. Zhong. Supported by the intramural program of the National Institute of Child Health and Human Development and grants from the American Cancer Society (M.Z.), the Karolinska Institute (F.A.), and the Wennergren Foundation (F.A.).

3 September 1997; accepted 6 January 1998